A SPIDER-INSPIRED ELECTROSPINNING FOR FABRICATION OF POLYVINYLIDENE FLUORIDE NANOFIBER MEMBRANES

by

Lei ZHAO[a,b,c*], Ting ZHU[c], Qianwen WANG[c], Li WEI[c], Jumei ZHAO[c], and Jun WANG[d]

[a] Textile and Clothing College, Yancheng Polytechnic College, Yancheng, China
[b] College of Textile and Clothing Engineering, Soochow University, Suzhou, China
[c] National Engineering Laboratory for Modern Silk, Soochow University, Suzhou, China
[d] Guangdong Wonder Testing International Co., Ltd., Guangzhou, China

Original scientific paper
https://doi.org/10.2298/TSCI2403251Z

This paper is to mimic the long transporting process of proteins in the spider spinning, and a long and helical needle electrospinning technology is proposed, the polyvinylidene fluoride solution is used to study the effects of needle helix spirals on the micromorphology, mechanical property, electrical property, porosity, and hydrophobic property of polyvinylidene fluoride nanofiber membranes. The results showed that there is a threshold value for the helix spirals helical pitch, and its spider-inspired mechanism is discussed.

Key words: *electrostatic spinning, nanofiber membrane, biomimetic design, spider*

Introduction

Spider silk has many advantages in light weight, high elasticity and good flexibility, which are incomparable to any artificial materials [1-4], and the long transport tube plays an important role in controlling the spinning process and silk properties [5]. Nature-inspired fabrication of nanofibers has triggered off enormous interest in materials science, for examples, proteins derived from mussels [6], latex [7], silkworms [8], spiders [9], sea-silk [10], and snails [11] were used for spinning nanofibers by the electrospinning technology or the bubble electrospinning. Liu *et al.* [12] suggested a general strategy of electrospinning for fabrication of microspheres, He *et al.* [13] gave a mathematical model for controlling the electrospinning process, and Wang *et al.* [14] revealed that unsmooth nanofibers can be used for energy harvesting. The bubble electrospinning is to use the polymer bubbles for fabrication of nanofibers and nanoscale membranes [15-17].

According to this special and amazing transporting property in the spider spinning process, Tian *et al.* [18-21] offered a total new angle to mimic the property using a long needle in the electrospinning process, their experiment showed that macromolecules and nanoparticles distribution in the inside of the nanofiber can be adjusted by the needle length. The macromolecular chains in the long tube can be gradually straightened and ordered, and when its length is long enough, all macromolecular chains have a tend to be straightened and

* Corresponding author, e-mail: zhaolei7365@163.com

aligned, so that the internal structure of the nanofibers can be controlled, as a result, the nanofiber properties can be greatly enhanced. Though much achievement has been made. The long needle electrospinning device take too much space, this paper suggests a modification using a long and helical needle to save space. Additionally, the protein solution in the spider spinning process has high viscosity, to mimic this property, The polyvinylidene fluoride (PVDF) [22] solution with high viscosity is used in experiment to verify our biomimetic design.

Materials and methods

Raw materials and reagents

Polyvinylidene fluoride (PVDF, molecular weight) was provided by Shanghai McLean Biochemistry Co. Ltd., dimethylformamide (DMF, analytically pure) was bought from Shanghai Aladdin Biochemical Technology Co., Ltd.

Preparation of PVDF nanofiber membranes

Nanofiber membranes were prepared by a modified electrospinning with a long and helical needle. He DMF was used as solvent to prepare PVDF/DMF solution with a mass fraction of 15% according to a standard process as that given in [18-21]. The solution was cooled to the environmental temperature and was injected into a 10 mL syringe, a combination of long needle and a spiral needle was used to transport the spun solution as illustrated in fig. 1, the long needle had a length of 150 mm, while the number of the helix spirals changed from 0 to 22. The inner diameter the both needles was 0.7 mm, and the injection speed of spun solution was unchanged, that was 1.1 mL per hour, the receipt distance was 18 cm, and the static voltage was 18 kV.

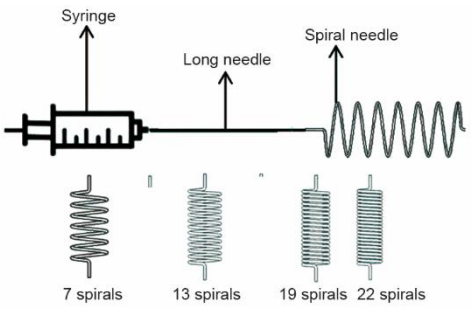

Figure 1. The transporting system with a long needle and a spiral needle

Performance characterization

The morphology of the obtained nanofiber membrane was characterized by the SEM (JSM-IT100, Japan Electronics Co., Ltd.), and the diameter of single nanofiber was tested by IMAGJ software (National Institute of Mental Health, USA). Instron-3365 (American Instron Company) was used to test the tensile properties and top breaking properties of the nanofiber membrane. The pore of nanofiber membrane was measured by automatic pore meter, POROMETER 3G, Andong Pa (Shanghai) Trading Co., Ltd., and the porosity was obtained by the gravimetric analysis. The electronic resistivity of the nanofiber membrane was characterized by a resistance tester (FT-400AHXM, Ningbo Ruike Weiye Instrument Co. Ltd.). A water drop angle tester (PZ-300SD, Beijing Pinzhi Chuangsi Precision Instrument Co. Ltd.) was used to measure the water contact angle of the spun nanofiber membrane.

Results and discussions

Surface morphology of nanofiber membranes

The SEM of PVDF nanofiber membrane was shown in fig. 2, and the diameter of PVDF nanofibers was measured, the results were listed in tab. 1.

Table 1. The PVDF nanometers with different spiral numbers

Number of helix spirals	Average diameter [nm]	Standard deviation [nm]	Confidence interval [nm]
0	117	±18.2	±3.6
7	178	±29.4	±5.3
13	135	±27.2	±4.4
19	110	±25.5	±3.7
22	98	±20.7	±3.1

From fig. 2 and tab. 1, it is obvious that the high viscous PVDF/DMF solution could be spun to different morphologies of the nanofibers according the different numbers of helix spirals. The nanofibers saw a tendency of decreasing average diameter with the increase of the number of helix spirals, though there was an inverse effect when the number was less than 7. This phenomenon was explained by the laminar flow theory in fluid mechanics as that discussed in [18-21].

Tensile and bursting properties of nanofiber membranes

In order to further characterize the effect of the number of helix spirals on mechanical properties, we measured the tensile and bursting properties of PVDF nanofiber membranes. The test results were illustrated in fig. 3.

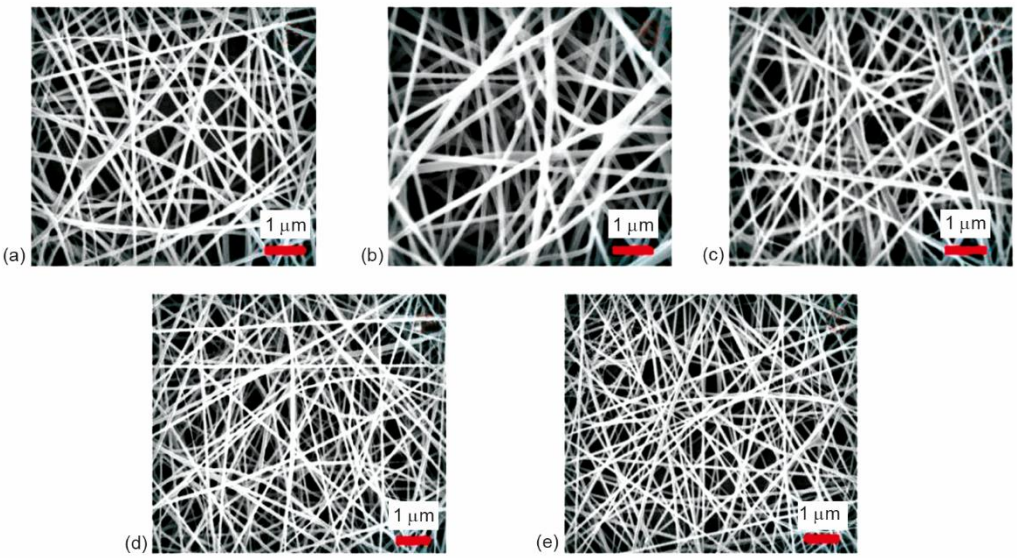

Figure 2. The SEM image of PVDF nanofiber membrane with different helix spirals; (a) 0, (b) 7, (c) 13, (d) 19, and (e) 22

From fig. 3(a), we found that the tensile stress increased from 5.37 MPa to 8.62 MPa when the number of helix spirals changed from 0 to 13, a 60.5% increase. While the fracture strain increased from 0.21% to 0.92%, a 338% increase. However, when the number of helix spirals increased from 13 to 22, the tensile stress and the fracture strain decreased sharply.

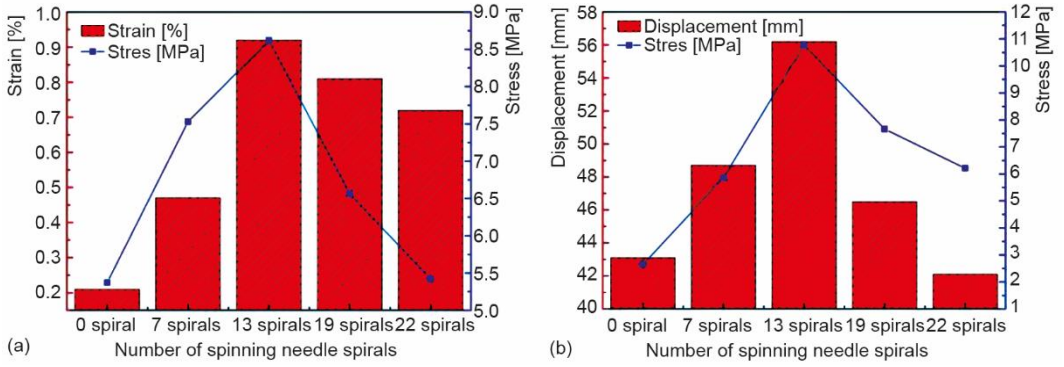

Figure 3 Mechanical properties of PVDF nanofiber membranes obtained by different numbers of helix spirals; (a) tensile stress-strain relationship and (b) toppling displacement-stress relationship

From fig. 3(b), it could be seen that when the number of helix spirals changed from 0 to 22, the tip break and displacement of the PVDF nanofiber membrane increased first and then decreased, and the maximum was at 13 helix spirals, the maximal tip break and the maximal displacement of the PVDF nanofiber membrane reached, respectively,10.78 MPa and 56.2 mm.

Electrical properties of nanofiber membranes

The PVDF nanofiber membrane resistance was measured and the results were listed in tab. 2. It could be clearly seen from tab. 2 that the electrical resistivity firstly increased and then decreased with the increase of the number of helix spirals. The electrical resistivity reached the maximum of 3.97×10^{13} Ωm when the number was 7. While the electrical conductivity decreased first and then increased, and its maximum of 4.81×10^{-14} S/m was reached when the number was 22. The change of the nanofiber membrane resistance or the conductivity depended upon the internal micro/nanostructure, especially crystallinity. When the number of helix spirals was not enough to adjust PVDF macromolecules regularly, PVDF macromolecules were distributed in a non-uniform form. When the spiral number increased, the twisting of PVDF macromolecules resulted in a more and more ordered micro/nano- inner structure, and PVDF macromolecules were distributed in a more uniform form, as a result, the electronic charge could be more easily transferred, so the electrical conductivity became higher.

Table 2. The resistance of PVDF nanofiber membranes obtained by different spiral numbers

Number of helix spirals	Resistance [Ωm]	Conductivity [Sm^{-1}]
0	3.20×10^{13}	3.13×10^{-14}
7	3.97×10^{13}	2.52×10^{-14}
13	3.77×10^{13}	2.65×10^{-14}
19	2.85×10^{13}	3.50×10^{-14}
22	2.08×10^{13}	4.81×10^{-14}

Pore analysis of nanofiber membranes

The PVDF nanofiber membrane pore distribution was shown in fig. 4 and listed in tab. 3.

Table 3. Pore size of PVDF nanofiber membrane prepared with different spiral numbers

Number of helix spirals	Pore distribution [μm]	Average diameter [μm]	Pore numbers	Porosity [%]
0	0.549~0.916	0.729	8.48×10^8	76.76
7	0.937~1.139	1.088	4.39×10^8	50.42
13	0.738~0.921	0.849	6.75×10^8	59.92
19	0.593~0.775	0.731	1.032×10^9	72.68
22	0.549~0.795	0.694	1.407×10^9	79.31

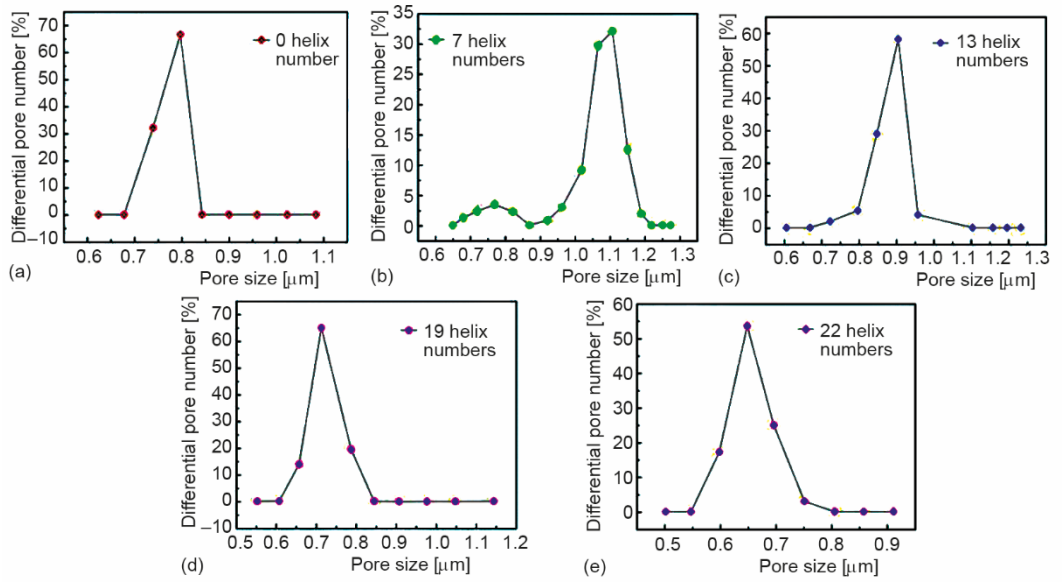

Figure 4. Pore distribution of PVDF nanofiber membrane prepared with different helix spirals

From tab. 3 and fig. 4, it is found that when the number of helix spirals increased from 0 to 7, the pore size distribution became significantly wider, the pore size increased also significantly, but the pore numbers decreased sharply, so the porosity decreased significantly as well. When the number of helix spirals increased further, the average pore size of the PVDF nanofiber membrane became narrower and narrower. When the number was 22, the pore number and porosity reached the maximum, which were 1.407×10^9 and 79.31%, respectively. The previously pore results were mainly caused by the change of the PVDF nanofibers diameter. The smaller diameter of PVDF nanofibers results in more pores.

Surface hydrophobicity of the nanofiber membrane

The diameter distribution and water contact angle of PVDF nanofiber membranes were shown in fig. 5. It could be intuitively seen from fig. 5 that when the helix spirals was 0, the diameter distribution of PVDF nanofibers was narrow, and the PVDF nanofiber membrane presented high hydrophobicity (the contact angle was about 135°). When the number was 7, the diameter distribution of PVDF nanofibers widened, and its hydrophobicity de-

creased. When the spiral number increased further, the diameter distribution of PVDF nanofibers narrowed. When the number was 22, the PVDF nanofibers had the narrowest diameter distribution and the best hydrophobicity (the contact angle was about 150°), which indirectly proved that the more uniform diameter of the nanofibers results in the better hydrophobic effect. The surface hydrophobicity can be explained by the geometrical potential theory [23, 24]. Nanofibers with smaller diameter have higher geometrical potential (surface energy), the average diameter of nanofibers obtained by 22 helix spirals was 98 nm, while that for zero helix spirals was 117 nm, so the contact angle of nanofiber membrane obtained by 22 helix spirals was larger than that by zero helix spirals.

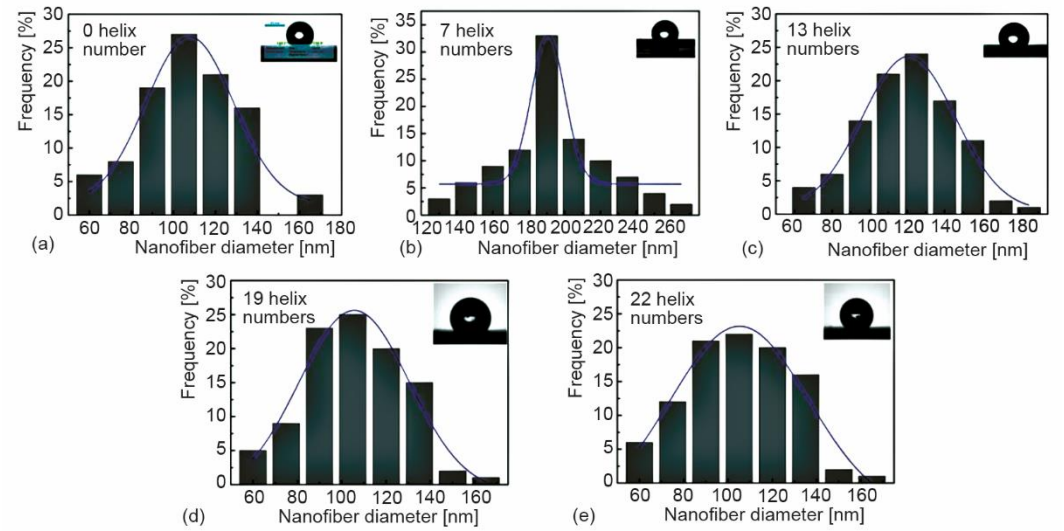

Figure 5. Diameter distribution and water contact angle of PVDF nanofibers prepared with different helix spirals

Conclusion

The change of the number of the helix spirals of the needle has an obvious effect on the micromorphology, mechanical properties, electrical properties, porosity and hydrophobic properties of PVDF nanofiber membranes. The phenomenon can be explained by the laminar flow theory [18-21] and the nanoscale fluid mechanics [25-27]. The ability to control or adjust the PVDF nanofibers properties by the helix spirals offers a totally new chance for various advanced applications, especially in energy harvesting devices [28, 29], wearable electronics [30] and nano/microelectromechanical (N/MEMS) systems [31-34]. Future research includes the deep learning system [35] to deal with the experimental data.

Acknowledgment

This research was funded by Jiangsu Higher Vocational College Teachers' Professional Leaders' High and Training Team Visit Project (Grant number: 2022TDFX008), Qing Lan Project of Jiangsu Colleges and Universities for Excellent Teaching Team in 2023 (Letter from the Faculty Department of Jiangsu Provincial Department of Education, 2023, No. 27), and Scientific Research Fund of Yancheng Polytechnic College (ygy2302). Jiangsu Province Higher Vocational Education High-level Major Group Construction Project-Modern Textile

Technology Major Group (Grant number: Jiangsu Vocational Education 2020. No 31), Brand Major Construction Project of International Talent Training in Colleges and Universities-Modern Textile Technology Major (Grant number: Jiangsu Foreign Cooperation Exchange Education 2022. No 8), and Key technology innovation platform for flame retardant fiber and functional textiles in Jiangsu Province (2022JMRH-003) all supported this research.

References

[1] Heim, M., *et al.*, Spider Silk: From Soluble Protein to Extraordinary Fiber, *Angewandte Chemie International Edition, 48* (2009), 20, pp. 3584-3596
[2] Cranford, S. W., *et al.*, Non-linear Material Behaviour of Spider Silk Yields Robust Webs, *Nature, 482* (2012), 7383, pp. 72-76
[3] Osaki, S., Spider Silk As Mechanical Lifeline, *Nature, 384* (1996), 6608, pp. 419-419
[4] Salehi, S., *et al.*, Spider Silk for Tissue Engineering Applications, *Molecules, 25* (2020), 3, 737
[5] Zuo, Y. T., Liu, H. J., Is the Spider a Weaving Master or a Printing Expert? *Thermal Science, 26* (2022), 3B, pp. 2471-2475
[6] Tian, D., *et al.*, Electrospun Mussel-derived Silk Fibers, *Recent Patents on Nanotechnology, 14* (2020), 1, pp. 14-20
[7] Zhou, C. J., *et al.*, Fabrication of Latex-based Nanofibers by Electrospinning, *Recent Patents on Nanotechnology, 13* (2019), 3, pp. 202-205
[8] Zhou, C. J., *et al.*, Silkworm-Based Silk Fibers by Electrospinning, *Results in Physics, 15* (2019), 102646
[9] Yu, D. N., *et al.*, Wetting and Supercontraction Properties of Spider-Based Nanofibers, *Thermal Science, 23* (2019), 4, pp. 2189-2193
[10] Tian, D., *et al.*, Sea-silk Based Nanofibers and their Diameter Prediction, *Thermal Science, 23* (2019), 4, pp. 2253-2256
[11] Yu, D. N., *et al.*, Snail-based Nanofibers, *Materials Letters, 220* (2018), June, pp. 5-7
[12] Liu, L. G., *et al.*, Dropping in Electrospinning Process: A General Strategy for Fabrication of Microspheres, *Thermal Science, 25* (2021), 2B, pp. 1295-1303
[13] He, C. H. , *et al.*, Taylor Series Solution for Fractal Bratu-type Equation Arising in Electrospinning Process, *Fractals, 28* (2020), 1, 2050011
[14] Wang, Q. L., *et al.*, Intelligent Nanomaterials for Solar Energy Harvesting: From Polar Bear Hairs to Unsmooth Nanofiber Fabrication, *Frontiers in Bioengineering and Biotechnology, 10* (2022), 926253
[15] Li, X. X., He, J.-H., Bubble Electrospinning with an Auxiliary Electrode and an Auxiliary Air Flow, *Recent Patents on Nanotechnology, 14* (2020), 1, pp. 42-45
[16] He, J.-H., *et al.* The Maximal Wrinkle Angle During the Bubble Collapse and Its Application to the Bubble Electrospinning, *Frontiers in Materials, 8* (2022), 800567
[17] Qian, M. Y., He, J.-H. Collection of Polymer Bubble as a Nanoscale Membrane, *Surfaces and Interface, 28* (2022), 101665
[18] Tian, D., He, J.-H., Macromolecular Electrospinning: Basic Concept & Preliminary Experiment, *Results in Physics, 11* (2018), Dec., pp. 740-742
[19] Tian, D., *et al.*, Macromolecule Orientation in Nanofibers, *Nanomaterials, 8* (2018), 11, 918
[20] Tian, D., He, J.-H., Self-assemble of Macromolecules in a Long and Narrow Tube, *Thermal Science, 22* (2018), 4, pp. 1659-1664
[21] Tian, D., He, J.-H., Macromolecular-scale Electrospinning: Controlling Inner Topologic Structure Through a Blowing Air, *Thermal Science, 26* (2022), 3B, pp. 2663-2666
[22] Li, X. X., *et al.*, Boosting Piezoelectric and Triboelectric Effects of PVDF Nanofiber Through Carbon-Coated Piezoelectric Nanoparticles for Highly Sensitive Wearable Sensors, *Chemical Engineering Journal, 426* (2021), 130345
[23] Peng, N. B., He, J.-H., Insight into the Wetting Property of a Nanofiber Membrane by the Geometrical Potential, *Recent Patents on Nanotechnology, 14* (2020), 1, pp. 64-70
[24] Li, X. X., *et al.*, High Energy Surface as a Receptor in Electrospinning: A Good Switch for Hydrophobicity to Hydrophilicity, *Thermal Science, 25* (2021), 3B, pp. 2205-2212
[25] He, J.-H., Elazem, N. Y. A., The Carbon Nanotube-Embedded Boundary Layer Theory for Energy Harvesting, *Facta Universitatis Series: Mechanical Engineering, 20* (2022), 2, pp. 211-235
[26] Kou, S. J., *et al.*, Fractal Boundary Layer and Its Basic Properties, *Fractals, 30* (2023), 9, 22501729

[27] Kumar, K., *et al.*, Irreversibility Analysis in Al_2O_3-Water Nanofluid Flow with Variable Property, Facta Universitatis Series: Mechanical Engineering, *Facta Universitatis Series: Mechanical Engineering, 20* (2022), 3, pp. 503-518
[28] Fan, F. R., *et al.*, Flexible Nanogenerators for Energy Harvesting and Self-Powered Electronics, *Advanced Materials, 28* (2016), 22, pp. 4283-4305
[29] He, C. H., *et al.*, Controlling the Kinematics of a Spring-Pendulum System Using an Energy Harvesting Device, *Journal of Low Frequency Noise, Vibration & Active Control, 41* (2022), 3, pp. 1234-1257
[30] Hwang, B., *et al.*, Bending Fatigue Behavior of Ag Nanowire/Cu Thin-Film Hybrid Interconnects for Wearable Electronics, *Facta Universitatis Series: Mechanical Engineering, 20* (2022), 3, pp. 553-560
[31] He, C. H., A Variational Principle for a Fractal Nano/Microelectromechanical (N/MEMS) System, *International Journal of Numerical Methods for Heat & Fluid Flow, 33* (2023), 1, pp. 351-359
[32] Skrzypacz, P., *et al.*, Dynamic Pull-in and Oscillations of Current-Carrying Filaments in Magnetic Micro-Electro-Mechanical System, *Communications in Nonlinear Science and Numerical Simulation, 109* (2022), 106350
[33] Tian, D., *et al.*, Fractal N/MEMS: from Pull-in Instability to Pull-in Stability, *Fractals, 29* (2021), 2, 2150030
[34] He, J.-H., *et al.*, Pull-in Stability of a Fractal MEMS System and Its Pull-in Plateau, *Fractals, 30* (2022), 9, 2250185
[35] Wang, S. Q., *et al.*, An Ensemble-Based Densely-Connected Deep Learning System for Assessment of Skeletal Maturity, *IEEE Transactions on Systems, Man, and Cybernetics: Systems, 52* (2020), 1, pp. 426-437

Paper submitted: December 1, 2022
Paper revised: March 11, 2023
Paper accepted: March 12, 2023